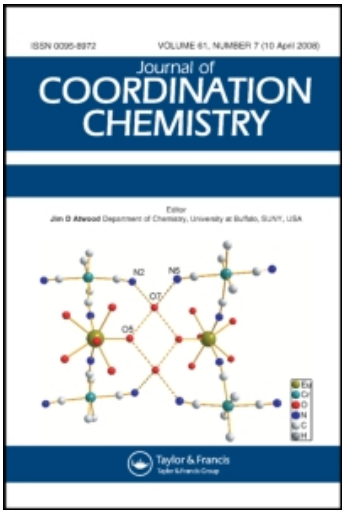


**Journal of Coordination Chemistry**
Publication details, including instructions for authors and subscription information:
http://www.informaworld.com/smpp/title~content=t713455674

# Synthesis, spectral and pharmacological studies on lanthanide(III) complexes of 3,5-pyrazoledicarboxylic acid

Irena Kostova[a]; Georgi Momekov[b]
[a] Faculty of Pharmacy, Department of Chemistry, Medical University, Sofia 1000, Bulgaria [b] Faculty of Pharmacy, Department of Pharmacology and Toxicology, Medical University, Sofia 1000, Bulgaria

**To cite this Article** Kostova, Irena and Momekov, Georgi(2008) 'Synthesis, spectral and pharmacological studies on lanthanide(III) complexes of 3,5-pyrazoledicarboxylic acid', Journal of Coordination Chemistry, 61: 23, 3776 — 3792
**To link to this Article: DOI:** 10.1080/00958970802155321
**URL:** http://dx.doi.org/10.1080/00958970802155321

*Journal of Coordination Chemistry*
Vol. 61, No. 23, 10 December 2008, 3776–3792

Taylor & Francis
Taylor & Francis Group

# Synthesis, spectral and pharmacological studies on lanthanide(III) complexes of 3,5-pyrazoledicarboxylic acid

IRENA KOSTOVA*† and GEORGI MOMEKOV‡

†Faculty of Pharmacy, Department of Chemistry, Medical University,
2 Dunav St., Sofia 1000, Bulgaria
‡Faculty of Pharmacy, Department of Pharmacology and Toxicology,
Medical University, 2 Dunav St., Sofia 1000, Bulgaria

(*Received 17 January 2008; in final form 19 March 2008*)



Complexes of cerium(III), lanthanum(III) and neodymium(III) with 3,5-pyrazoledicarboxylic acid ($H_3$pdc) were synthesized and their compositions determined by elemental analysis. To identify the binding of Ce(III), La(III) and Nd(III) with $H_3$pdc, detailed vibrational analysis was performed comparing experimental vibrational spectra of the ligand and its Ln(III) complexes with theoretically predicted and with literature data from related compounds. Significant differences in the IR and Raman spectra of the complexes were observed as compared to spectra of the ligand. The ligand and the complexes were tested for cytotoxic activities on the chronic myeloid leukemia derived K-562, overexpressing the BCR-ABL fusion protein and the non-Hodgkin lymphoma derived DOHH-2, characterized by an overexpression of the antiapoptotic protein bcl-2 cell lines. The results indicate that the tested compounds exerted considerable cytotoxic activity upon the evaluated cell lines in a concentration dependent manner; we constructed dose-response curves and calculated corresponding $IC_{50}$ values. The lanthanide complexes exhibited potent cytotoxic activity, even more than cisplatin towards K-562 and DOHH-2 cell lines. In order to elucidate some of the mechanistic aspects of the observed cytotoxic effects, we evaluated whether the established cytotoxicity of the most active complex La($H_2$pdc) is related to its capacity to induce cell death through apoptosis.

*Keywords*: Lanthanide complexes; 3,5-Pyrazoledicarboxylic acid; IR- and Raman-spectra; Cytotoxic activity; DNA

## 1. Introduction

New metal complexes with 3,5-pyrazoledicarboxylic acid ($H_3$pdc) have attracted attention due to the interesting properties of $H_3$pdc, including access to the six coordination sites controlled by varying the pH, allowing control over the synthesis of coordination polymers using various metal centers [1, 2]. A series of M(II) complexes with $H_3$pdc has been synthesized *via* hydrothermal reactions [3]. Simple mononuclear

*Corresponding author. Email: irenakostova@yahoo.com

*Journal of Coordination Chemistry*
ISSN 0095-8972 print/ISSN 1029-0389 online © 2008 Taylor & Francis
DOI: 10.1080/00958970802155321

[M(II) = Co(II), Zn(II) and Cu(II)] and dinuclear building blocks have been isolated [4]. Hydrothermal reactions of simple alkaline salts or their hydroxides with $H_3$pdc yielded new coordination compounds at different pH levels [5]; increase in pH resulted in a higher connectivity of the ligand, which in turn leads to a higher dimensionality of the crystal structures. Coordination polymers of $UO_2^2$ have been prepared and characterized by single-crystal X-ray diffraction, thermogravimetric analyses (TGA) and fluorescence spectroscopy [6]. Rare-earth metal coordination polymers have also been obtained, e.g. ($[Eu_2(Hpdc)_3(H_2O)_6]$ [7]. Lanthanide atom sizes (the lanthanide contraction) directly control the type of structure formed by coordination of a single 3,5-pyrazoledicarboxylic acid [8].

$H_3$pdc can use its carboxylate oxygen and pyrazole nitrogen atoms, which are highly accessible to metals, to form both monodentate and/or multidentate M–O and M–N bonds. The structural motifs thus generated can readily form hydrogen-bonded networks [9, 10]. This ligand possesses three different protonated hydrogens ($H_a$, $H_b$, and $H_c$ in figure 1). The difference in these protons allows them to deprotonate at different pH levels. The flexible, multifunctional coordination sites also give likelihood for generation of coordination polymers with high dimensions. "Harder" lanthanide metals coordinate preferably to oxygen, while "softer" nitrogens bind to transition metals.



Although a variety of coordination polymers and complexes of $H_3$pdc containing transition metals have been synthesized, very few rare-earth metal complexes have been reported. Herein, we report a series of coordination systems containing rare-earth metals and discuss their antiproliferative activity. Little is known about cytotoxic activity of lanthanide(III) coordination compounds with $H_3$pdc. Our recently published studies on rare-earth metal coordination compounds involving biologically active ligands showed that a number of human tumor cell lines are very sensitive to lanthanide complexes and these metals have different cytotoxic profiles [11–20]. These promising results prompted our search for cytotoxic lanthanide complexes with 3,5-pyrazoledicarboxylic acid.

Thus, the aim of this work was to synthesize and characterize complexes of cerium(III), lanthanum(III) and neodymium(III) with 3,5-pyrazoledicarboxylic acid and to determine the cytotoxic activities of these complexes in *in vitro* tumor test systems as chronic myeloid leukemia derived K-562, overexpressing the BCR-ABL fusion protein and the non-Hodgkin lymphoma derived DOHH-2, characterized by an overexpression of the antiapoptotic protein bcl-2 cell lines.

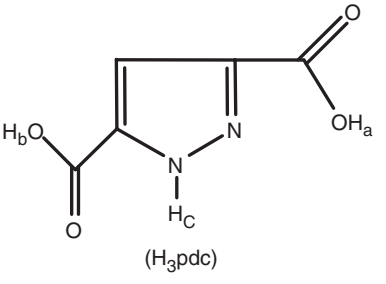


Figure 1. The structure of the ligand 3,5-pyrazoledicarboxylic acid.

## 2. Experimental

### 2.1. *Chemistry*

The compounds used for preparing the solutions were Merck products, p.a. grade: $Ce(NO_3)_3 \cdot 6H_2O$, $La(NO_3)_3 \cdot 6H_2O$ and $Nd(NO_3)_3 \cdot 6H_2O$. 3,5-Pyrazoledicarboxylic acid was used as a ligand for preparation of metal complexes (figure 1).

**2.1.1. Physical and spectroscopic measurements.** Carbon, hydrogen and nitrogen contents of the compounds were determined by elemental analysis. The water content was determined by Metrohn Herizall E55 Karl Fisher Titrator.

The solid-state infrared spectra of the ligands and their complexes were recorded in KBr from 4000–400 $cm^{-1}$ by FT-IR 113V Bruker spectrometer, in Nujol by IR-spectrometer FTIR-8101M Shimadzu and in the range 700–200 $cm^{-1}$ by IR-spectrometer Perkin-Elmer GX Auto image system.

The Raman spectra of the compounds were recorded with a Dilor Labram microspectrometer (Horiba-Jobin-Yvon, model LabRam) equipped with a 1800 grooves $mm^{-1}$ holographic grating. The 514.5 nm line of an argon ion laser (Spectra Physics, model 2016) was used for the probe excitation. The spectra were collected in a backscattering geometry with a confocal Raman microscope equipped with an Olympus LMPlanFL 50x objective and with a resolution of 2 $cm^{-1}$. The detection of Raman signal was carried out with a Peltier-cooled CCD camera. Laser power of 100 mW was used in our measurements.



**2.1.2. General method of synthesis.** The complexes were synthesized by reaction of cerium(III), lanthanum(III) and neodymium(III) salts, and the ligand in molar ratio of 1 : 2. Different ratios (1 : 1, 1 : 2, 1 : 3) were tried, but in all cases the product had composition 1 : 2. The complexes were prepared by adding an aqueous solution of cerium(III), lanthanum(III) and neodymium(III) salt to an aqueous solution of the ligand and raising the pH of the mixture gradually to ca 5.0 by adding dilute sodium hydroxide. The reaction mixture was stirred with an electromagnetic stirrer at 25°C for one hour. At the moment of mixing the solutions, precipitates were obtained. The precipitates were filtered (pH of the filtrate was 5.0), washed several times with water and dried in a desiccator to constant weight. The complexes were insoluble in water, methanol and ethanol and soluble in DMSO.

### 2.2. *Pharmacology*

In the present study we investigated the cytotoxic effects of the three newly synthesized lanthanide complexes using the standard MTT-dye reduction assay for cell viability. The cytotoxic effects of the tested lanthanide complexes were assessed on the chronic myeloid leukemia derived K-562, overexpressing the BCR-ABL fusion protein and the non-Hodgkin lymphoma derived DOHH-2, characterized by an overexpression of the antiapoptotic protein bcl-2 cell lines. In order to elucidate some of the mechanistic aspects of the observed cytotoxic effects, we evaluated whether the established cytotoxicity of the most active complex $La(H_2pdc)$ is related to its capacity to induce cell death through apoptosis.

**2.2.1. Cell culture maintenance, drug solutions and treatment.** The cell culture flasks and the 96-well microplates were obtained from NUNCLON (Denmark). MTT, FCS and cisplatin were purchased from Sigma Co.

In this study the cell lines were grown as suspension-type cultures in a controlled environment, RPMI 1640 medium (Sigma), with 10% heat inactivated fetal bovine serum (Sigma) and 2mM L-glutamine (Sigma), in a ''Heraeus'' incubator with humidified atmosphere and 5% carbon dioxide, at 37°C. In order to maintain the cells in log phase, cell suspension was discarded two or three times per week and the cell culture was re-fed with fresh RPMI-1640 aliquots.

The stock solutions of tested compounds (20 mM) were freshly prepared in DMSO, and thereafter, diluted in RPMI-1640 medium in order to achieve the desired final concentrations. The serial dilutions of tested compounds were prepared immediately before use. At the final dilutions, the concentration of DMSO never exceeded 1%. The solutions were stored at 4°C, protected from light for a maximum of 1 week. The cell culture maintenance, the drug solution preparation, as well as the treatment procedures, were performed in a ''Heraeus'' Laminar flow cabinet.



**2.2.2. Cell viability determination (MTT assay).** The cell viability was determined using the MTT-dye reduction assay. Briefly, exponentially growing cells were seeded in 96-well microplates (100 μL well$^{-1}$) at a density of $1 \times 10^5$ cells per mL; after 24 h incubation at 37°C they were exposed to various concentrations of the lanthanide complexes for 48 h. After the incubation with the test compounds MTT solution (10 mg mL$^{-1}$ in PBS) was added (10 μL well$^{-1}$). The plates were further incubated for 4 h at 37°C and the formazan crystals formed were dissolved through addition of 100 μL well$^{-1}$ 5% solution of formic acid in 2-propanol (Merck). The absorption of the samples was then measured using an ELISA reader (Uniscan Titertec) at 580 nm. The blank solution consisted of 100 μL RPMI 1640 medium (Sigma), 10 μL MTT stock and 100 μL 5% formic acid in 2-propanol. The survival fractions were calculated as percentage of the untreated control using the formula:

$$\mathrm{SF}\% = \frac{A_{\mathrm{test}}}{A_{\mathrm{control}}} \times 100$$

where $A_{\mathrm{test}}$ is the average value for the absorption at a given concentration and $A_{\mathrm{control}}$ is the average absorption of the untreated control, respectively.

**2.2.3. Apoptosis assay.** The oligonucleosomal fragmentation of genomic DNA, which is characteristic for the apoptotic process, was detected using a 'Cell Death Detection' ELISA kit (Roche Diagnostics, Germany). K-562 cells were exposed to equitoxic concentrations ($IC_{50}$) of La($H_2$pdc) or cisplatin for 24 h. Cytosolic fractions of $1 \times 10^4$ cells per group (treated or untreated) served as an antigen source in a sandwich ELISA, utilizing primary anti-histone antibody-coated microplate and a secondary peroxidase-conjugated anti DNA-antibody. The photometric immunoassay for histone-associated DNA fragments was executed using a microprocessor-controlled microplate reader (Labexim LMR-1). The results were expressed as the oligonucleosome enrichment factor (representing a ratio between the absorption in the treated versus the untreated control samples).

Table 1. Elemental analysis of Ln(III) complexes of 3,5-pyrazoledicarboxylic acid.

| Compound formula | Calculated/Found (%) | | | | |
|---|---|---|---|---|---|
| | C | H | N | $H_2O$ | Ln |
| $Ce(H_2pdc)_2(OH)\cdot 4H_2O$ | 20,86/20,80 | 2,61/2,67 | 9,74/9,85 | 12,52/12,05 | 24,35/23,93 |
| $La(H_2pdc)_2(OH)\cdot 4H_2O$ | 20,90/20,79 | 2,61/2,64 | 9,76/9,75 | 12,54/12,08 | 24,22/23,87 |
| $Nd(H_2pdc)_2(OH)\cdot 4H_2O$ | 20,72/20,71 | 2,59/2,41 | 9,67/10,16 | 12,43/12,15 | 24,87/24,56 |

$H_3pdc = C_5H_4N_2O_2$; $H_2pdc = C_5H_3N_2O_2^-$.

**2.2.4. Statistics.** The data processing included the Student's *t*-test with $p \leq 0.05$ taken as significance level using Microsoft EXCEL for PC, and the plots were generated using Microcal Origin, version 3.5.

## 3. Results and discussion

### 3.1. *Chemistry*

The compositions of the new complexes were characterized by elemental analysis. The metal ions were determined after mineralization. The water content in the complexes was determined by Karl Fisher analysis. The elemental analyses and the results of the Karl Fisher analysis are presented in table 1.

In the syntheses, the ligand was first deprotonated with sodium hydroxide and the corresponding anionic species are active in reaction with lanthanide ions. The $H_c$ in this ligand (figure 1) on the nitrogen of the pyrazole ring is more difficult to deprotonate than the two carboxylate protons. Thus, carboxylate oxygens are the preferred sites for coordination to Ln(III) ions. Although $H_a$ and $H_b$ are both attached to carboxylic oxygen atoms, $H_a$ can be deprotonated more easily, allowing the oxygen to form a chelating bond to a metal center. This will be checked by a detailed and comparative vibrational study of the ligand and its Ln(III) complexes.

### 3.2. *Vibrational analysis of $H_3$pdc and its Ce(III), La(III) and Nd(III) complexes*

The bonding of the ligand to Ce(III), La(III) and Nd(III) was elucidated by recording the IR and Raman spectra of the complexes as compared with those of the free ligand. The vibrational fundamentals from the IR and Raman spectra (figures 2 and 3) were analyzed by comparing these modes with those from the literature [21] in combination with the results of our DFT calculations (i.e., harmonic vibrational wavenumbers and their Raman scattering activities) [22]. In tables 2(a) and 2(b) selected, calculated and experimental IR and Raman data together with tentative assignments are given. All the calculated modes are numbered from the largest to the smallest frequency within each fundamental wavenumber. The last columns in tables 2(a) and 2(b) respectively show the approximate description of the normal modes according to the B3PW91 and B3LYP methods [22]. A survey of the last column shows that many vibrations are complex and involve strongly coupled motions. The assignments have been given by studying literature reports [23] and comparing the spectra of the ligand and of the

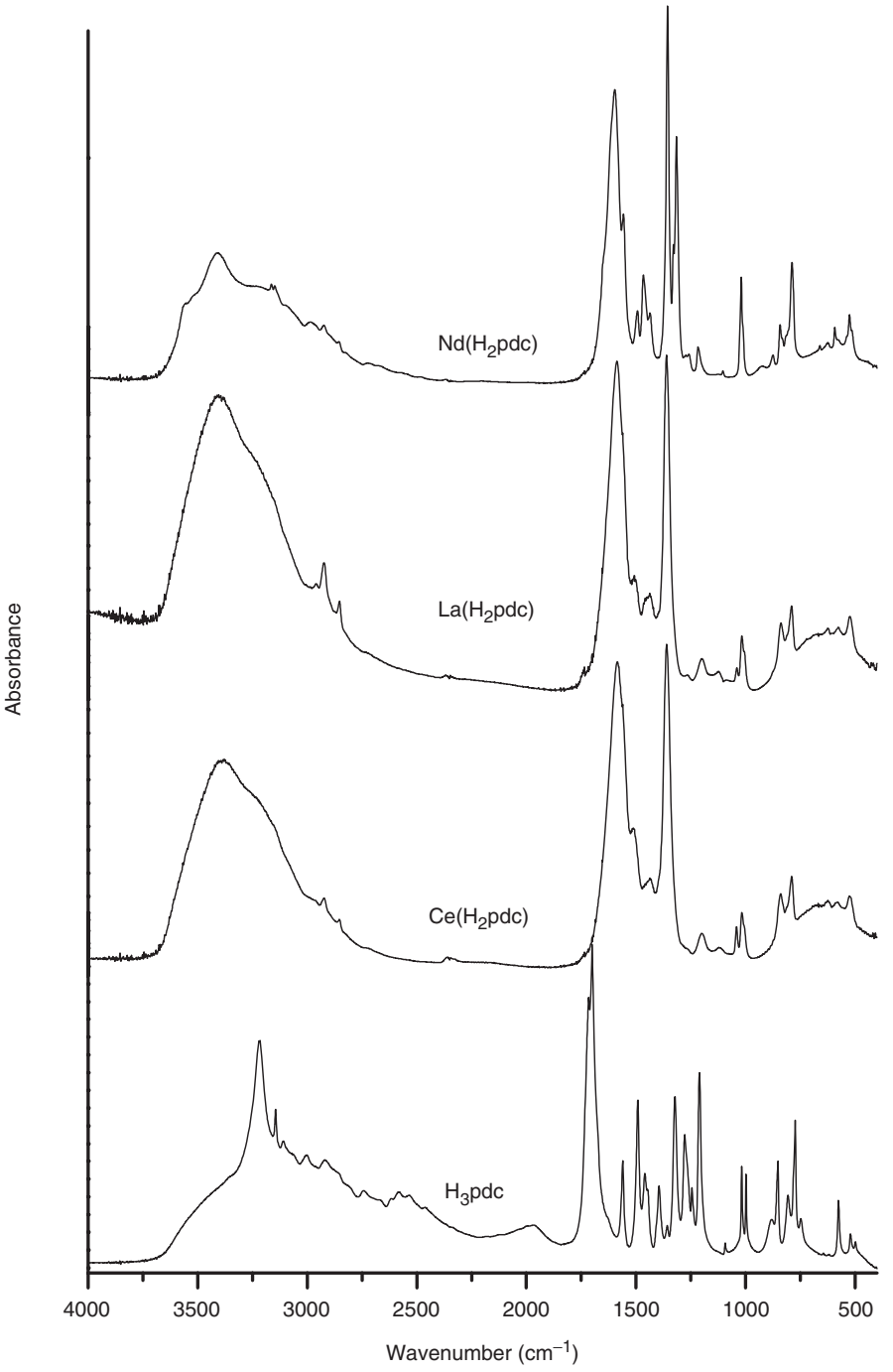


Figure 2. IR spectra of $H_3pdc$ and its Ce(III), La(III) and Nd(III) complexes.

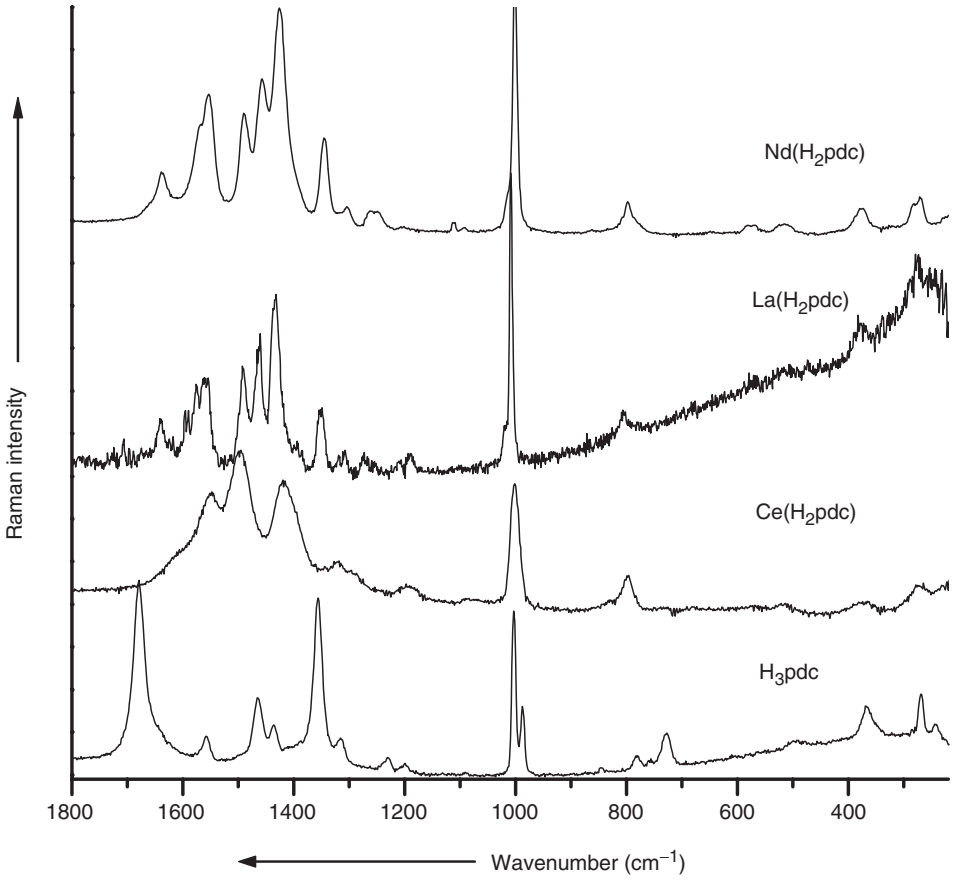


Figure 3. Raman spectra of solid state of $H_3$pdc and its Ce(III), La(III) and Nd(III) complexes. Excitation: 514.5 nm, 50 mW.



metal complexes. We emphasize that some stretching and deformation modes are coupled so that the proposed assignments should be regarded as approximate descriptions of the vibrations.

To illustrate the vibrational behavior of the ligand upon the metal coordination we present the FT-IR spectra in the 4000–500 $cm^{-1}$ range (figure 2), as well as the Raman spectra of the investigated compounds in the 1800–200 $cm^{-1}$ range (figure 3). Both the IR and the Raman spectra were considered for full description of the vibrational behavior of the investigated species. Below we discuss characteristic vibrational modes of the ligand changes upon complexation with Ln(III).

**3.2.1. O–H stretching modes, ν(OH).** According to the calculations, the IR band at 3220 $cm^{-1}$ for the ligand is assigned to the O–H stretching mode [22], shifted to lower wavenumbers due to intramolecular O···H–O bonds. In the $\nu$(OH)/$H_2O$ region the spectra of Ce(III), La(III) and Nd(III) complexes show one medium band at about 3230 $cm^{-1}$, attributed to coordinated water. This band overlaps with $\nu(NH_2)$.

Table 2(a). Calculated and experimental IR wavenumbers ($cm^{-1}$) of $H_3pdc$ and its Ce(III), La(III) and Nd(III) complexes and their tentative assignments.

| Calculated [22] | | | | Experimental | | | | |
|---|---|---|---|---|---|---|---|---|
| B3PW91 | | B3LYP | | | | | | |
| LANL2DZ | 6-311++G** | LANL2DZ | 6-311++G** | $H_3pdc$ | $Ce(H_2pdc)$ | $La(H_2pdc)$ | $Nd(H_2pdc)$ | Vibrational assignment |
| 3347 | | 3331 | | 3353 sh | 3378 s | 3405 vs | 3404 ms | $\nu$(NH) |
| | 3294 | | 3285 | 3220 s | 3228 sh | 3229 sh | | $\nu$(OH) |
| | | | | 3144 wm | 3165 sh | 3159 sh | 3163 wm | $\nu$(CH) |
| | | | | 3109 w | 3101 sh | | 3092 sh | $\nu$(CH) |
| | | | | 3064 sh | 3070 sh | 3088 sh | | $\nu$(CH) |
| | | | | 3002 w | 3003 sh | 2961 vw | 2984 w | $\nu$(=C–H) |
| | | | | 2920 w | 2924 vw | 2924 wm | 2924 w | $\nu$(CH) |
| | | | | 2876 sh | 2854 vw | 2853 w | 2855 w | $\nu$(C–C–H) |
| | | | | 1968 w | | | | $\nu_{asym}$(COO) |
| 1716 | | 1698 | | 1717 vs | | 1735 vw | | $\nu_{sym}$(COO) |
| 1710 | | 1692 | | 1700 vs | | | | $\nu_{asym}$(C=O) |
| | | | | 1633 sh | | | | $\nu_{sym}$(C=O) |
| 1601 | 1604 | 1585 | 1590 | 1560 m | 1585 vs | 1587 vs | 1596 s | $\nu_{sym}$(ring) |
| 1524 | 1519 | | 1501 | 1492 s | 1513 m | | 1494 w | $\delta_{ip}$(ring) |
| 1459 | 1476 | 1507 | 1457 | 1460 m | | 1508 m | 1467 m | $\nu$(N=N); $\nu$(ring) |
| 1436 | 1450 | 1440 | 1433 | | 1438 wm | | 1437 wm | $\nu$(ring) |
| 1375 | 1383 | 1420 | | 1395 sh | | 1438 m | | $\nu$(ring) |

(*continued*)

Table 2(a). Continued.

| Calculated [22] | | | | | | | | |
|---|---|---|---|---|---|---|---|---|
| B3PW91 | | B3LYP | | Experimental | | | | |
| LANL2DZ | 6-311++G** | LANL2DZ | 6-311++G** | $H_3$pdc | Ce($H_2$pdc) | La($H_2$pdc) | Nd($H_2$pdc) | Vibrational assignment |
| 1332 | 1350 | 1357 | 1363 | 1357 m | 1361 vs | 1361 vs | 1356 vs | $\nu$(ring); $\delta$ (C–OH) |
| 1332 | | 1320 | 1337 | 1322 s | | | 1315 s | $\nu$(C–O) |
| 1281 | 1288 | 1270 | 1279 | 1278 ms | | 1266 vw | 1272 w | $\delta_{op}$(CH) |
| 1222 | 1244 | | 1225 | 1244 m | | | | $\delta_{ip}$(CH); $\nu$(COC) |
| 1222 | 1188 | 1200 | 1181 | 1210 s | 1200 w | 1199 w | 1217 w | $\nu_{sym}$(C=O) |
| 1158 | 1168 | 1153 | 1152 | | | 1123 vw | | $\delta_{ip}$NH; $\nu$(ring) |
| 1081 | 1092 | 1090 | 1089 | 1094 w | 1043 m | 1041 w | 1104 vw | $\nu$(ring); $\nu$(CH) |
| 1021 | 1030 | 1012 | 1025 | 1018 m | 1017 m | 1017 wm | 1019 m | $\delta_{ip}$(CH); $\delta_{op}$ (CH); $\nu$(ring) |
| 984 | 998 | 976 | 994 | 998 m | | | | $\delta_{ip}$(ring) |
| | 884 | | 885 | 881 wm | | | 875 vw | $\delta_{op}$(CH); $\delta_{op}$ (ring) |
| | | | | 852 m | 840 m | 838 wm | 843 wm | $\delta_{op}$(CH) |
| 794 | 797 | 787 | 792 | 806 wm | 790 m | | 809 sh | $\delta_{op}$(CH) |
| 777 | 779 | 766 | 773 | 772 ms | | 790 m | 788 m | $\delta_{op}$(CH) |
| 771 | 733 | 759 | 773 | 747 wm | | | | $\delta_{op}$(CH) |
| 713 | 716 | 708 | 729 | | | 625 w | | $\delta$(OCO) |
| 585 | 571 | 579 | 609 | 577 m | 581 w | 578 w | 593 w | $\delta_{op}$(ring) |
| 555 | 552 | 552 | 547 | 522 w | 527 w | 524 w | 526 w | $\delta_{op}$(NH) |
| 495 | 504 | 492 | 502 | | 508 sh | | 515 sh | $\nu$(M-O) |
| 445 | 460 | 443 | 458 | 499 w | | 475 sh | 452 wv | $\delta$(OCO) |

Abbreviations: vw – very weak; w – weak; m – medium; ms – medium strong; s – strong; vs – very strong; sh – shoulder; $\nu$ – stretching; $\delta$ – bending; sym – symmetric; asym – asymmetric; ip – in-plane; op – out-of-plane; M – metal.

Table 2(b). Calculated and experimental Raman wavenumbers ($cm^{-1}$) of $H_3pdc$ and its Ce(III), La(III) and Nd(III) complexes and their tentative assignments.

| Calculated [22] | | | | Experimental solid | | | | |
|---|---|---|---|---|---|---|---|---|
| B3PW91 | | B3LYP | | | | | | |
| LANL2DZ | 6-311++G** | LANL2DZ | 6-311++G** | $H_3pdc$ | $Ce(H_2pdc)$ | $La(H_2pdc)$ | $Nd(H_2pdc)$ | Vibrational assignment |
| 3348 | | 3332 | | | | | 3417 vw | $\nu$(NH) |
| | 3295 | | 3285 | | | | | $\nu$(OH) |
| | | | | 3137 m | 3139 wm | 3160 sh | 3145 wm | $\nu$(CH) |
| | | | | 3111 w | | 3142 w | | $\nu$(CH) |
| | | | | 3071 w | | | 3071 w | $\nu$(CH) |
| | | | | | | | 1996 sh | $\nu_{asym}$(COO) |
| 1710 | | 1698 | | 1679 vs | | | | $\nu_{asym}$(C=O) |
| 1601 | | 1691 | | 1641 sh | 1620 sh | 1634 w | 1637 wm | $\nu_{sym}$(C=O) |
| 1524 | 1604 | 1585 | 1590 | 1558 w | 1549 s | 1570 sh | 1554 s | $\nu_{sym}$(ring) |
| | 1476 | 1507 | 1501 | | 1498 vs | | 1489 ms | $\delta_{ip}$(ring) |
| 1459 | 1450 | 1440 | 1457 | 1464 m | | 1458 m | 1457 s | $\nu$(N=N); $\nu$(ring) |
| 1436 | | 1420 | 1433 | 1436 w/m | 1418 s | 1426 s | 1426 vs | $\nu$(ring) |
| 1375 | | 1357 | 1363 | 1356 vs | | 1343 m | 1346 ms | $\nu$(ring); $\delta$(C–OH) |
| 1332 | 1350 | 1320 | 1337 | 1316 w | 1322 m | 1317 vw | 1305 w | $\nu$(C–O) |
| 1280 | 1288 | 1270 | 1279 | | 1299 sh | 1264 vw | | $\delta_{op}$(CH) |
| 1222 | 1244 | | 1225 | 1231 w | 1257 sh | | 1260 w | $\delta_{ip}$(CH); $\nu$(COC) |
| | 1188 | 1200 | 1181 | 1201 w | 1195 wm | | 1204 vw | $\nu_{sym}$(C=O) |
| 1158 | 1168 | 1153 | 1152 | 1133 vw | | | 1112 vw | $\delta_{ip}$ NH; $\nu$(ring) |
| 1081 | 1092 | 1090 | 1089 | 1090 vw | 1089 vw | | 1093 vw | $\nu$(ring); $\nu$(CH) |
| 1021 | 1030 | 1012 | 1025 | 1003 s | 1002 s | 1002 s | 1002 vvs | $\delta_{ip}$(CH); $\delta_{op}$(CH); $\nu$(ring) |
| 984 | 998 | 976 | 994 | 988 ms | | | | $\delta_{ip}$(ring) |
| | 884 | | 885 | 897 vw | | | | $\delta_{op}$(CH); $\delta_{op}$(ring) |
| | | | | 844 vw | 857 sh | | 863 vw | $\delta_{op}$(CH) |
| | 797 | 787 | 792 | | 798 m | | 798 wm | $\delta_{op}$(CH) |
| 794 | 779 | 766 | 773 | 782 vw | | 801 w | | $\delta_{op}$(CH) |
| 771 | | 759 | | 756 sh | | | | $\delta_{op}$(CH) |
| 713 | 733 | 708 | 729 | 729 w/m | 730 vw/680 | 654 vw | 648 vw | $\delta$(OCO) |
| 585 | 571 | 579 | 609 | 605 vw | 572 vw | 563 vw | 572 w | $\delta_{op}$(ring) |
| 555 | 552 | 552 | 547 | | 518 w | 513 vw | 515 w | $\nu$(M–O) |
| 323 | 328 | 322 | 326 | 366 m | 368 w | 343 vw | 376 wm | $\nu$(M–O) |
| 217 | 222 | 218 | 224 | | 210 wm | 224 sh | 212 sh | $\nu$(O–M–O) |

Abbreviations: vw – very weak; w – weak; m – medium; ms – medium strong; s – strong; vs – very strong; sh – shoulder; $\nu$ – stretching; $\delta$ – bending; sym – symmetric; asym – asymmetric; ip – in-plane; op – out-of-plane; M – metal.

The assignment of O–H and N–H stretching bands overlapped in the same spectral region is rather difficult, and the involvement of these groups in hydrogen bonds affects their wavenumbers and produces broadening in the IR and Raman spectra.

**3.2.2. Vibrational modes of the carbonylic C=O and carboxylic COOH groups.** The most informative for the metal-ligand binding mode in the Ln(III) complexes is the $\nu$(C=O). According to our DFT calculations [22], bands in the 1720–1630 $cm^{-1}$ region were assigned to the asymmetric and symmetric stretching vibration of the carboxylic and carbonylic groups. Some of these stretching modes are active in the IR spectra and others are active in the Raman spectra. The strong IR bands at 1717, 1700 and 1633 $cm^{-1}$ and the Raman bands at 1679 and 1641 $cm^{-1}$ were assigned to $\nu$(C=O) modes of the carboxylic and carbonylic groups in the ligand, respectively [tables 2(a) and 2(b)]. In general, strong peaks in the spectra of the complexes around 1600–1400 $cm^{-1}$ are characteristic of asymmetric and symmetric vibrations for uni and bidentate carboxylate groups. The difference, $\Delta\nu$, between the asymmetric and symmetric $COO^-$ stretching frequencies is greater in complexes than in simple salts. Bidentate binding of the $COO^-$ group in the complexes was suggested, as reported in the literature [8].The structure of the complexes is presented in figure 4.

According to our calculations [22], bands at 1322 (IR) and 1316 (Raman) $cm^{-1}$ for the ligand were assigned to $\nu$(C–O) with low intensity in the Raman spectra. The bands around 1200 $cm^{-1}$, weak in IR and very weak in Raman, were attributed to the asymmetrical C–O stretching and were slightly changed in the complexes.

**3.2.3. N–H and C–H stretching modes.** Stretching vibrations around 3500 $cm^{-1}$ in all spectra are attributed to secondary aromatic amine. In the 3600–2700 $cm^{-1}$ region the

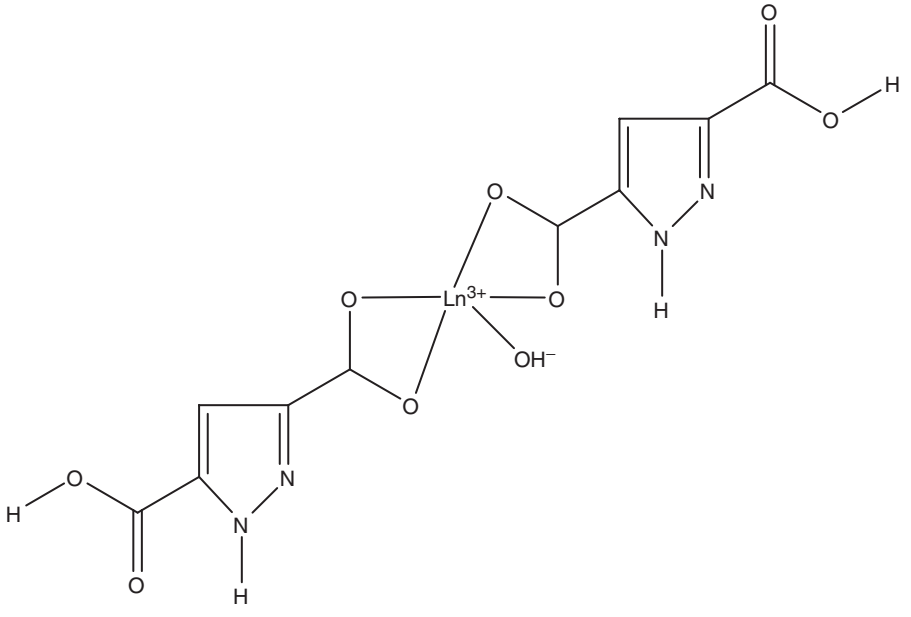


Figure 4. The proposed structure of the lanthanide(III) complexes with 3,5-pyrazoledicarboxylic acid.

N–H stretching mode is a shoulder at 3353 $cm^{-1}$ for $H_3pdc$, and a strong or medium strong band for the Ce complex (3378 $cm^{-1}$), La complex (3405 $cm^{-1}$) and Nd complex (3404 $cm^{-1}$). The out of plane NH bending modes in the IR spectra, $H_3pdc$ (522 $cm^{-1}$), Ce complex (527 $cm^{-1}$), La complex (524 $cm^{-1}$) and Nd complex (526 $cm^{-1}$) are absent in the Raman spectra. The absence of large systematic shifts of these bands in the spectra of the complexes implies that there is no interaction between the amino nitrogen and the lanthanide(III).

Bands around 3100 $cm^{-1}$ can be attributed to C–H stretching. The wavenumber region 2700–2500 $cm^{-1}$ in IR and Raman spectra is typical of strong hydrogen bonded intermolecular complexes due to a strong anharmonic coupling (Fermi resonance) of the NH stretching vibrations with overtones and combinations of lower frequency modes of the bonded molecules [22].

**3.2.4. Ring stretching modes, ν(CC).** Coordination of Ln(III) to the carboxylate oxygens affected to some extent the IR and Raman bands of pyrazole-ring modes. In the IR spectra of $H_3pdc$, and its Ce, La and Nd complexes, medium and very strong bands at 1560, 1585, 1587 and 1596 $cm^{-1}$ were assigned to the symmetric stretching mode of the pyrazole ring, while in Raman spectra this vibration is a weak peak at 1558 $cm^{-1}$ for the ligand, and strong bands at 1549, 1570 and 1554 $cm^{-1}$ for the Ce, La and Nd complexes, respectively. Other bands from pyrazol ring stretching modes in the IR spectra are at 1460, 1395, 1357 $cm^{-1}$ (for the $H_3pdc$), 1438, 1361 $cm^{-1}$ (for the Ce complex), 1438, 1361 $cm^{-1}$ (for the La complex) and 1437, 1356 $cm^{-1}$ (for the Nd complex), shifted to lower wavenumbers (tables 2a and 2b). The in-plane bending of the pyrazole ring can be observed at 1500 $cm^{-1}$ in the IR and Raman spectra for all componds; bands at 880 and 600 $cm^{-1}$ in the IR and Raman spectra can be assigned to out of plane pyrazole ring bending. Bands for the pyrazole-ring vibrations were not shifted significantly in the spectra of Ce(III), La(III) and Nd(III) complexes, indicating that Ln(III) did not produce substantial polarization on the pyrazole ring.



**3.2.5. CH bending modes, δ(CCH) and ring in-plane and out-of-plane deformations.** The CH in-plane bending modes, $\delta(CH)_{ip}$, were observed at their usual positions in the 1250–1020 $cm^{-1}$ region, stronger in the Raman than in the IR spectra. Medium IR bands in the 880–750 $cm^{-1}$ region were assigned to out-of-plane deformation vibrations of the hydrogen atoms in the ring, $\delta(CH)_{op}$. The bands due to the CH bending modes and to ring deformations are slightly changed in spectra of the complexes. The assignment of IR and Raman bands in this spectral range is difficult because highly coupled modes and combination bands overlap with those due to fundamentals, distorting the observed bands.

**3.2.6. Ln–O stretching and O–Ln–O bending modes.** The spectra in the region below 600 $cm^{-1}$ are particularly interesting since they provide information about the metal-ligand vibrations. The Raman spectra are particularly useful in studying the metal-oxygen stretching vibrations, with medium intensity bands that are weak in the infrared spectra.

New bands at about 510–520 $cm^{-1}$, which appear in the IR and Raman spectra of the Ce, La and Nd complexes, are due to metal-oxygen vibrations. In the low wavenumber

region in the Raman spectrum of $H_3$pdc (figure 3) we observe a medium band at 366 $cm^{-1}$, which is slightly shifted in Raman spectra of the Ce, La and Nd complexes and becomes weaker.

The metals interact with symmetric, bidentate carboxylate anions and both oxygen atoms of the carboxylate are symmetrically bonded to the metal. We observe in the Raman spectra of the Ce, La and Nd complexes bands at 210–220 $cm^{-1}$, perhaps due to O–M–O vibrations. Because of the predominant electrostatic character of the Ln–O bonding, the $\nu$(Ln–O) modes have low intensities and are coupled with other modes; hence, their assignment is very difficult. Our previous calculations [14] predict that bands due to $\nu(Ln–O)_{water}$ and $\nu(Ln–O)_{OH}$ should also appear about 200 $cm^{-1}$.

Unfortunately, we were not able to obtain suitable single crystals for X-ray diffraction determination of the crystal and molecular structure of the complexes studied. Therefore, molecular modeling of the molecular structure was used to suggest the type of the metal coordination. In our previous investigation, we performed an accurate density functional theory study (DFT) of the ligand [22]. The results showed the most probable site for metal binding are the carboxylate oxygens. Our IR and Raman spectral data confirmed that carboxylate oxygens coordinate to the metal ion. Thus, on the basis of the experimental and theoretical results, we suggest the metal ion coordinates to the carboxylate after deprotonation of Ha (figure 1). The other carboxylic groups of the ligands can coordinate with another metal ion, forming a polymeric structure in accord with previous published data on related compounds [7–10, 24].



### 3.3. *Pharmacology*

**3.3.1. *In vitro* cytotoxicity.** The screening performed revealed that all lanthanide complexes evaluated exerted cytotoxic effects against the chronic myeloid leukemia derived K-562, overexpressing the BCR-ABL fusion protein and the non-Hodgkin lymphoma derived DOHH-2, characterized by an overexpression of the antiapoptotic protein bcl-2 cell lines in a concentration dependent manner, which enabled construction of concentration response curves (a sample is shown in figure 5; all are in Supplementary Material), tables 3–6. The corresponding Ln(III) nitrate salts were inactive in the investigated concentration range [11–20].

The newly reported compounds inhibit the proliferation of K-562 cells significantly, outclassing cisplatin in terms of the $IC_{50}$ values obtained. Indeed this CML-derived cell line is characterized via a high expression of the fusion protein BCR-ABL [25], which is a constitutive non-receptor tyrosine kinase rendering K-562 less responsive to chemotherapeutic agents and other pro-apoptotic stimuli [26]. Unlike cisplatin, however, the cytotoxic efficacy of the novel complexes was not influenced by the BCR-ABL over expression and caused 50% inhibition of the malignant cell growth at substantially lower concentrations than cisplatin.

Even more intriguing discrepancy between the cytotoxic efficacy of the lanthanide complexes and cisplatin was encountered in DOHH-2 cells. Notwithstanding the practically equivalent relative potencies (in terms of $IC_{50}$) the new complex compounds caused almost total eradication of DOHH-2 within the higher concentrations exploited, while the efficacy of cisplatin reached a plateau with more than 30% viable cells even at the highest concentration exploited (200 μM), generally ascribed to the well-established

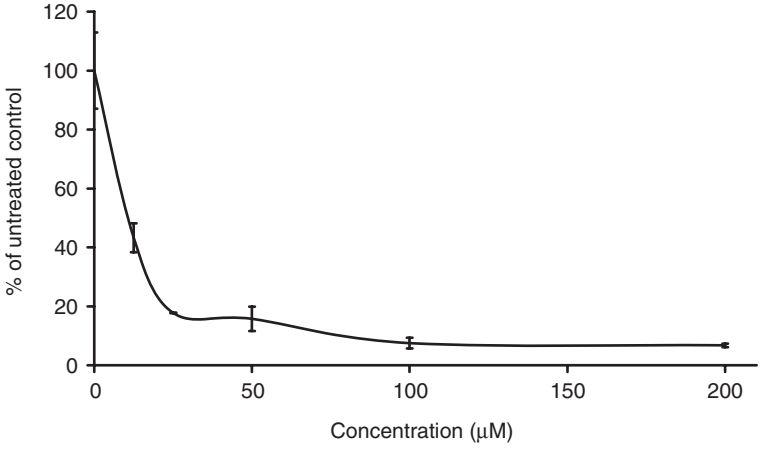


Figure 5. Cytotoxic effects of $Ce(H_2pdc)_2(OH) \cdot 4H_2O$ on the chronic myeloid leukemia-derived K-562 cell line after 48 h exposure, as assessed by the MTT-dye reduction assay. Each data point represents the mean ± SD ($n \geq 6$).



Table 3. Spectrophotometric data from the MTT assay concerning the cytotoxic effects of the compounds on K–562 cells.

| | MTT-formazan absorption at 580 nm | | | | | |
|---|---|---|---|---|---|---|
| Cell line | Untreated control | 12.5 μM | 25 μM | 50 μM | 100 μM | 200 μM |
| $C_5H_4N_2O_2$ | 0.48 ± 0.04 | 0.40 ± 0.02 | 0.46 ± 0.03 | 0.37 ± 0.02 | 0.42 ± 0.01 | 0.20 ± 0.02 |
| $Ce(H_2pdc)_2(OH) \cdot 4H_2O$ | 0.62 ± 0.08 | 0.110 ± 0.001 | 0.110 ± 0.001 | 0.10 ± 0.02 | 0.05 ± 0.01 | 0.04 ± 0.004 |
| $La(H_2pdc)_2(OH) \cdot 4H_2O$ | 0.62 ± 0.08 | 0.25 ± 0.02 | 0.07 ± 0.01 | 0.06 ± 0.01 | 0.05 ± 0.03 | 0.05 ± 0.005 |
| $Nd(H_2pdc)_2(OH) \cdot 4H_2O$ | 0.62 ± 0.08 | 0.29 ± 0.01 | 0.07 ± 0.01 | 0.05 ± 0.01 | 0.04 ± 0.02 | 0.04 ± 0.01 |
| Cisplatin | 0.81 ± 0.04 | 0.73 ± 0.03 | 0.57 ± 0.05 | 0.23 ± 0.02 | 0.18 ± 0.02 | 0.09 ± 0.03 |

Table 4. Spectrophotometric data from the MTT assay concerning the cytotoxic effects of the compounds on DOHH-2 cells.

| | MTT-formazan absorption at 580 nm | | | | | |
|---|---|---|---|---|---|---|
| Cell line | Untreated control | 12.5 μM | 25 μM | 50 μM | 100 μM | 200 μM |
| $C_5H_4N_2O_2$ | 0.25 ± 0.02 | 0.10 ± 0.01 | 0.09 ± 0.01 | 0.09 ± 0.01 | 0.09 ± 0.003 | 0.000 |
| $Ce(H_2pdc)_2(OH) \cdot 4H_2O$ | 1.13 ± 0.07 | 0.38 ± 0.02 | 0.24 ± 0.06 | 0.18 ± 0.06 | 0.09 ± 0.03 | 0.05 ± 0.01 |
| $La(H_2pdc)_2(OH) \cdot 4H_2O$ | 1.13 ± 0.07 | 0.32 ± 0.07 | 0.19 ± 0.08 | 0.07 ± 0.03 | 0.04 ± 0.02 | 0.03 ± 0.03 |
| $Nd(H_2pdc)_2(OH) \cdot 4H_2O$ | 1.23 ± 0.12 | 0.46 ± 0.06 | 0.40 ± 0.06 | 0.13 ± 0.07 | 0.05 ± 0.02 | 0.05 ± 0.01 |
| Cisplatin | 1.26 ± 0.07 | 0.49 ± 0.05 | 0.45 ± 0.05 | 0.45 ± 0.04 | 0.46 ± 0.04 | 0.40 ± 0.06 |

high level of bcl-2 expression in DOHH-2 cells [25]. This anti-apoptotic protein abolishes several of the cell-death signaling pathways, which are involved in the cytotoxic action of cisplatin, and conversely higher levels of bcl-2 are well established to confer resistance to platinum-based drugs [27–29]. The superior inhibition of DOHH-2

Table 5. Relative potency of the investigated compounds in the panel of human tumor cell line K-562, following 48 h treatment cells.

| Compound | $IC_{50}$ value |
|---|---|
| $C_5H_4N_2O_2$ | >200 μM |
| $Ce(H_2pdc)_2(OH)\cdot 4H_2O$ | 11.01 μM |
| $La(H_2pdc)_2(OH)\cdot 4H_2O$ | 10.50 μM |
| $Nd(H_2pdc)_2(OH)\cdot 4H_2O$ | 11.74 μM |
| Cisplatin | 36.68 μM |

Table 6. Relative potency of the investigated compounds in the panel of human tumor cell line DOHH-2, following 48 h treatment cells.

| Compound | $IC_{50}$ value |
|---|---|
| $C_5H_4N_2O_2$ | 12 μM |
| $Ce(H_2pdc)_2(OH)\cdot 4H_2O$ | 9.44 μM |
| $La(H_2pdc)_2(OH)\cdot 4H_2O$ | 8.75 μM |
| $Nd(H_2pdc)_2(OH)\cdot 4H_2O$ | 9.92 μM |
| Cisplatin | 10.25 μM |



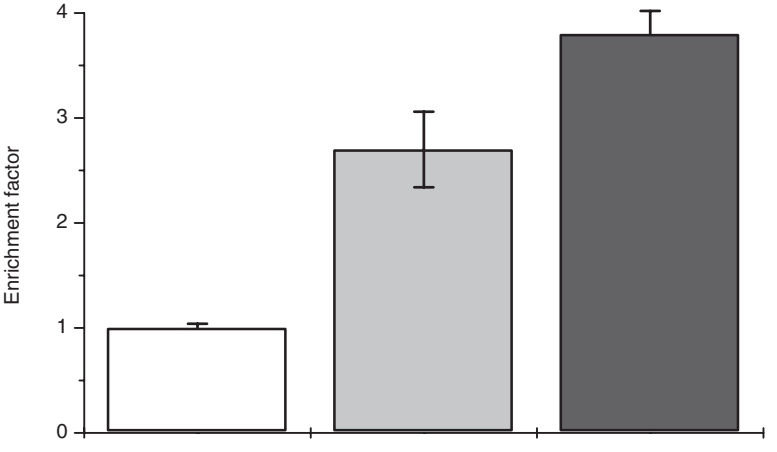


Figure 6. Cytosolic enrichment of K-562 with oligonucleosomal DNA fragments, following a 24 h exposure to equitoxic concentrations ($IC_{50}$) of cisplatin (gray column) or $La(H_2pdc)$ (black column) *vs*. the untreated control (white column). The results represent the arithmetic means (±SD) of four independent experiments.

proliferation by the lanthanide compounds implies that this class of tumor-inhibiting metal coordination compounds bypass the bcl-2 mechanisms of cellular resistance.

**3.3.2. Apoptosis induction.** The ability of anticancer agents to recruit the apoptotic cell death signaling pathways plays a crucial role in their cytotoxic mode of action. We evaluated whether the established cytotoxicity of $La(H_2pdc)$ is related to its capacity to induce cell death through apoptosis. Thus, the level of oligonucleosomal DNA fragmentation following 24 h exposure was monitored using a commercially available ELISA-kit. As evident from the results summarized in figure 6, both the most active

complex La($H_2$pdc) and cisplatin led to significant enrichment of K-562 cytosole with mono- and oligonucleosomal DNA fragments, whereby the fragmentation of genomic DNA was even more prominent after exposure to the lanthanum complex.

We have previously reported that the cytotoxicity of diverse lanthanide complexes is mediated through apoptosis induction and the results from this study corroborate the generality of this phenomenon. The prominent proapoptotic activity of La($H_2$pdc) in K-562 is of special interest, taking into account the fact that this cell line is characterized via the strong expression of the non-receptor protein kinase BCR-ABL which endows them with low responsiveness to diverse proapoptotic stimuli, including chemotherapeutic agents.

## 4. Conclusions

The vibrational properties of 3,5-pyrazoledicarboxylic acid and its Ln(III) complexes have been investigated by FT-Raman and FT-IR spectroscopies and supported by previously published theoretical calculations [22]. The difference between observed and calculated wavenumber values of most of the fundamental modes is very small. Vibrational evidence for bidentate coordination of carboxylic oxygens to the Ce(III), La(III) and Nd(III) ions was found. On the basis of the above detailed vibrational study we were able to suggest the most probable structural formula of the investigated complexes (figure 4).

All of the newly synthesized Ln(III) complexes exhibited cytotoxic activity in micromolar concentrations. These results confirmed our previous observations on the cytotoxicity of lanthanide(III) complexes as well as on their possible mechanism of action. Taken together the results from the cytotoxicity screening suggest that lanthanide(III) complexes with 3,5-pyrazoledicarboxylic acid, being very active cytotoxic agents, necessitate further pharmacological evaluation.



## References

[1] N. Ching, L. Pan, X.Y. Huang, J. Li. *Acta Crystallogr. C*, **56**, 1124 (2000).
[2] A.M. Beatty, K.E. Granger, A.E. Simpson. *Chem. Eur. J.*, **8**, 3254 (2002).
[3] L. Pan, N. Ching, X. Huang, J. Li. *Chem. Eur. J.*, **7**, 4431 (2001).
[4] P. King, R. Clérac, C.E. Anson, A.K. Powell. *Dalton Trans.*, **6**, 852 (2004).
[5] L. Pan, T. Frydel, M.B. Sander, X. Huang, J. Li. *Inorg. Chem.*, **40**, 1271 (2001).
[6] M. Frisch, C.L. Cahill. *Dalton Trans.*, **8**, 1518 (2005).
[7] L. Pan, X. Huang, J. Li, Y. Wu, N. Zheng. *Angew. Chem.*, **112**, 537 (2000).
[8] L. Pan, X. Huang, J. Li, Y. Wu, N. Zheng. *Angew. Chem. Int. Ed.*, **39**, 527 (2000).
[9] L. Pan, X. Huang, J. Li. *J. Solid State Chem.*, **152**, 236 (2000).
[10] L. Pan, N. Ching, X. Huang, J. Li. *Inorg. Chem.*, **39**, 5333 (2000).
[11] I. Kostova, G. Momekov. *Appl. Organomet. Chem.*, **21**, 226 (2007).
[12] I. Kostova, V.K. Rastogi, W. Kiefer, A. Kostovski. *Appl. Organomet. Chem.*, **20**, 483 (2006).
[13] I. Kostova, I. Manolov, I. Nicolova, S. Konstantinov, M. Karaivanova. *Eur. J. Med. Chem.*, **36**, 339 (2001).
[14] I. Georgieva, I. Kostova, N. Trendafilova, V.K. Rastogi, G. Bauer, W. Kiefer. *J. Raman Spectrosc.*, **37**, 742 (2006).
[15] I. Kostova, I.I. Manolov, G. Momekov. *Eur. J. Med. Chem.*, **39**, 765 (2004).
[16] I. Kostova, N. Trendafilova, G. Momekov. *J. Inorg. Biochem.*, **99**, 477 (2005).
[17] I. Kostova, G. Momekov, M. Zaharieva, M. Karaivanova. *Eur. J. Med. Chem.*, **40**, 542 (2005).

[18] I. Kostova, R. Kostova, G. Momekov, N. Trendafilova, M. Karaivanova. *J. Tr. Elem. Med. Biol.*, **18**, 219 (2005).
[19] I. Kostova, N. Trendafilova, T. Mihailov. *Chem. Phys.*, **314**, 73 (2005).
[20] I. Kostova, V.K. Rastogi, W. Kiefer, A. Kostovski. *Arch. Pharm. Pharm. Med. Chem.*, **339**, 598 (2006).
[21] S.D. Robinson, M.F. Utley. *J. Chem. Soc., Dalton Trans.*, 1914 (1973).
[22] N. Peica, I. Kostova, W. Kiefer. *Chem. Phys.*, **325**, 411 (2006).
[23] V.R. Thalladi, M. Nusse, R. Boese. *J. Am. Chem. Soc.*, **122**, 9227 (2000).
[24] X.H. Li. *Acta Crystallogr. E*, **61**, m2329 (2005).
[25] H.G. Drexler, W. Dirks, R.A.F. MacLeod, H. Quentmeier, K. Steube, C.C. Uphoff (Eds.). *DSMZ Catalogue of Human and Animal Cell Lines*, 6th Ed., DSMZ GmbH, Braunschweig (1997).
[26] H.G. Drexler, A.F. Roderick, C. McLeod, C. Uphoff. *Leuk. Res.*, **23**, 207 (1999).
[27] S. Akiyama, Z. Chen, T. Sumizawa, T. Furukawa. *Anti-Cancer Drug Des.*, **14**, 143 (1999).
[28] T. Miyashita, J.C. Reed. *Blood*, **81**, 151 (1993).
[29] T.C. Fisher, A.E. Milner, C.D. Gregory. *Cancer Res.*, **53**, 3321 (1993).